Journal of Physics: Condensed Matter

Effect of impurities on the successive phase transitions in $(Cs_{1-x}Rb_x)_2ZnI_4$ compounds

To cite this article: I P Aleksandrova *et al* 2002 *J. Phys.: Condens. Matter* **14** 13623

INSTITUTE OF PHYSICS PUBLISHING JOURNAL OF PHYSICS: CONDENSED MATTER

J. Phys.: Condens. Matter **14** (2002) 13623–13634 PII: S0953-8984(02)39800-X

Effect of impurities on the successive phase transitions in $(Cs_{1-x}Rb_x)_2ZnI_4$ compounds

I P Aleksandrova[1], J Bartolomé[2], L R Falvello[2], J M Torres[2] and A A Sukhovskii[1]

[1] L V Kirenski Institute of Physics, Russian Academy of Sciences, Siberian Branch, 660036 Krasnoyarsk, Russia
[2] Instituto de Ciencia de Materiales de Aragón, CSIC-Universidad de Zaragoza, 50009 Zaragoza, Spain

Received 19 July 2002
Published 29 November 2002
Online at stacks.iop.org/JPhysCM/14/13623

Abstract

The heat capacity, nuclear quadrupole resonance (NQR) and x-ray diffraction of $(Cs_{1-x}Rb_x)_2ZnI_4$ single crystals have been measured, for $x = 0$, 0.001, 0.005, 0.01, 0.025 and 0.05. The normal to incommensurate (N–Inc) phase transition at T_I, the incommensurate to commensurate (Inc–C) lock-in transition at T_L and the structural commensurate monoclinic to triclinic transition at T_{LT}, observed in the parent compound ($x = 0$), takes place for $x = 0$, 0.001, 0.005 and 0.01. For $x = 0.025$ only T_I and T_L are detected, while for $x = 0.05$ no transitions were observable. The values of T_I and T_L increase with x while T_{LT} decreases and disappears at the concentration $x = 0.025$. The effect of defects, besides modifying the transition temperatures, is that of broadening and lowering the heat capacity anomaly at the lock-in transition until its total quenching for $x = 0.05$. No observable hysteresis is detected in this transition. NQR and x-ray diffraction data show the Inc–C transition up to the highest concentration. We conclude that this phenomenology is caused by weak interaction of the incommensurate modulation with point defects even in the region close to the Inc–C transition.

1. Introduction

The incommensurate phase in ideal crystals is a degenerate state which has a gapless phason mode in the oscillation spectrum. Defects induce a gap in the phason branch as has been shown by various authors in both theoretical models and experimental measurements. The interaction of the modulation with defects in models was studied in two different regimes. In the first case a strong field of defects is assumed and the modulation phase at the defect location is determined only by the defect (strong pinning condition) [1]. The system possesses a large number of metastable states in one- and three-dimensional models in both the sinusoidal and the soliton lattice limits (see for example [2–4]). In the second case the collective field

of all defects determines the modulation phase. The influence of the defects is accounted for through the randomization of interactions ('weak-pinning condition') [1]. This regime has been less studied. The incommensurate structure here is not so obviously unstable with respect to defects, except probably in the very close vicinity of the lock-in transition, where the intersoliton interaction falls down.

In crystals, as a matter of fact, some intermediate cases are realized. In the well studied crystals of the A_2BX_4 family a number of regularly observed phenomena were understood on the basis of these model approximations. The thermal hysteresis of the incommensurate–commensurate (Inc–C) transition strongly increases with point defect concentration [5]. In ion-substituted crystals the thermal hysteresis region may reach ∼50 K, which is near one-half of the incommensurate phase interval [6]. In the hysteresis region the coexistence of metastable modulations with different wavevectors (q_Δ) or very pronounced steplike behaviour of q_Δ were observed by means of x-ray and neutron diffraction [7–9].

The solid solutions $(Cs_{1-x}Rb_x)_2ZnI_4$ as well as the parent crystal Cs_2ZnI_4 belong to the A_2BX_4 family with the *Pnma* space group in the normal (N) phase. In earlier studied nuclear quadrupole resonance (NQR) measurements we did not observe any hysteresis of the Inc–C transition up to the largest concentration of Rb ions, $x = 0.025$, studied [10]. Besides, we measured the heat capacity of a sample with a small Rb content ($x = 0.0018$), and observed that it already caused important effects on the lock-in anomaly height. The unexpected lack of hysteresis and the strong effect of defects on the lock-in transition has stimulated us to investigate in more detail these series.

In the present paper we have performed the calorimetric (section 2.1), the NQR (section 2.2) and the x-ray measurements (section 2.3) of the solid solution system $(Cs_{1-x}Rb_x)_2ZnI_4$ in the range of concentrations $0 < x < 0.05$. The thermodynamic analysis of the heat capacity is done in section 3. In section 4 it is concluded that the present series corresponds to the case of weak interaction of the incommensurate modulation with point defects.

2. Experimental results

The $(Cs_{1-x}Rb_x)_2ZnI_4$ crystals were grown by the Bridgeman method in quartz ampoules with an argon ambient. The starting reagents, Cs_2ZnI_4 and Rb_2ZnI_4, were purified by repeated recrystallization. The Rb content was controlled *a posteriori* by plasma absorption and x-ray fluorescence.

2.1. Heat capacity

To perform the heat capacity experiments the samples were cut as thin slabs of approximately 0.2 mm width and 2 mg weight. Then one face was painted black to enhance light absorption. The heat capacity measurements were performed using a Sinku-Riku ACC-1VL calorimeter between 77.4 and 280 K. The frequency used for the excitation signal was 2 Hz. Two runs, one heating and another cooling were performed for each sample to study the existence of thermal hysteresis. Several measurements have been carried out at heating rates of 5 and 15 K h^{-1} to extrapolate to zero rate and thus obtain the transition temperature determination near equilibrium.

For each compound the non-anomalous baseline was calculated by naive interpolation of the data over ($T > 130$ K) and below ($T < 84$ K) the transition region, by a second-order polynomial fitted by the least-squares method. The anomalous excess heat capacity $\Delta C_p(T)$ was calculated by direct difference between $C_{\exp}(T)$ and the obtained baseline. Because of

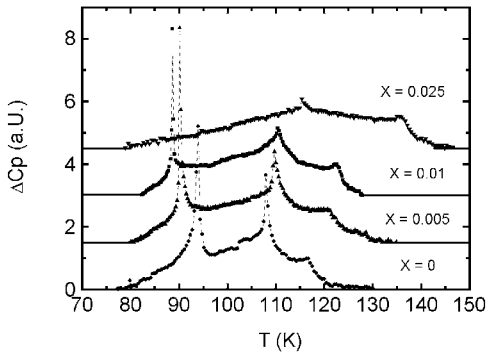

Figure 1. Temperature dependence of the anomalous heat capacity of the solid solutions $(Cs_{1-x}Rb_x)_2ZnI_4$ ($x = 0$, 0.005, 0.01 and 0.025). Note the ordinate origins are shifted for the different x. The thick line is the baseline to be interpolated.

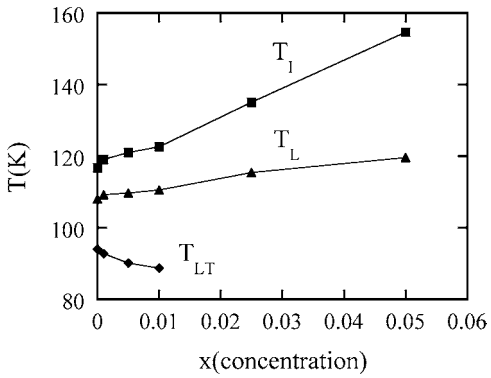

Figure 2. Evolution of the transition temperatures T_I, T_L and T_{LT} of $(Cs_{1-x}Rb_x)_2ZnI_4$ as a function of Rb content (x) from heat capacity data.

the relative character of the heat capacity, for comparison reasons the excess heat capacity in the anomalous region was normalized to the height of the anomaly at the N–Inc transition; i.e. $\Delta C_p(T_I) = 1$.

The heat capacity curves at the concentration of the substituted ions in the range $0 \leqslant x \leqslant 0.05$ are shown in figure 1. At small concentrations $x = 0.001$, 0.005 and 0.01 three anomalies existing in the pure compound at T_I (N–Inc), T_L (Inc–C) and T_{LT} (low temperature) also appear. The values of T_I and T_L increase with x while T_{LT} decreases. The variation of the anomalous temperatures depends linearly on x (see figure 2). The measured values of T_I and T_L in figure 2 are in all cases about 5 K lower than those determined from NQR measurements [10], while the first-order transition temperature T_{LT} coincides. This difference is connected with a specific behaviour of the NQR spectra in the transition region [10] preventing to determine precisely the transition temperature.

While the general aspect of the anomaly at T_I is similar in all the cases, the peak at T_L decreases in height and broadens. The difference in transition temperature between the warming and cooling runs was in all cases measured as less than 0.2 K for $x = 0.005$ and 0.01. For $x = 0.025$ the uncertainty increases to 0.5 K.

In all measured cases the heat capacity in the region between T_L and T_{LT} depends linearly on temperature. By fitting a straight line we have extrapolated the commensurate heat capacity

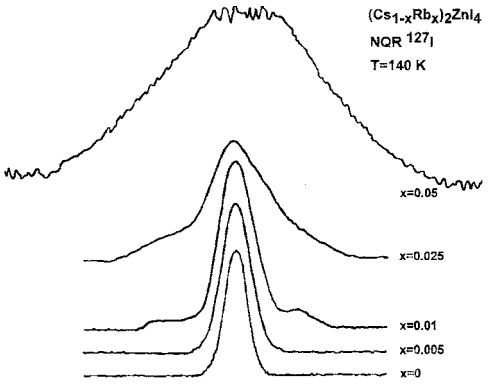

Figure 3. The shape of the ^{127}I NQR line centred at 77.5 MHz of $(Cs_{1-x}Rb_x)_2ZnI_4$ at $x = 0$, 0.005, 0.01, 0.025 and 0.05 [10].

Table 1. Transition temperatures, heat capacity peak at the L transition and fit parameters r, α^* and T_0 for the measured $(Cs_{1-x}Rb_x)_2ZnI_4$ compounds.

	$x = 0$	$x = 0.0011$	$x = 0.005$	$x = 0.01$	$x = 0.025$	$x = 0.05$
T_I (K)	116.7	119.1	121	122.6	135	154.6
T_L (K)	108	109.2	109.7	110.5	115.4	119.6
T_C (K)	94	92.7	90.14	88.7	—	—
$\Delta C_p(T_L)$	1.85	1.67	1.59	1.60	1.28	—
$r(x)$	0.50	0.45	0.42	0.45	0.33	—
$\alpha^*(x)$	−3.2	−3.9	−4.3	−3.8	−5.9	
$T_0(x)$	114.7	117	119	120	132	

up to T_L and have calculated the excess heat capacity $\Delta C(T_L)$ as the anomalous heat capacity just below T_L. The results are given in table 1, where the progressive reduction of $\Delta C(T_L)$ is evidenced. The delta peak at T_{LT} is sharp and first order for all x.

In contrast to the lower concentrations, in the $x = 0.025$ crystal only the N–Inc and Inc–C transitions are detected, as can be seen from figure 1. In fact, the transition at T_L had to be ascertained from the phase shift between the crystal temperature and the power applied to it. This sample seems different from the less doped ones, namely in the absence of the first-order transition at T_{LT} and in the near suppression of the transition at T_L. Nevertheless, the linear dependence of T_L on x is still fulfilled. In the sample with $x = 0.05$ any indications of the transitions were absent. With the phase shift technique only a tenuous hint of the anomaly at T_I could be recognized.

2.2. NQR

We have used the NQR method on the ^{127}I lines to determine the character of the Rb ion distribution in the substituted crystals. At small concentrations the Gaussian broadening of the NQR lines at $T = 140$ K, i.e. in the normal phase (figure 3), indicates a random distribution of defects. However already at $x = 0.01$ one may detect the appearance of very broad weak lines on both sides of the N-phase line. At $x = 0.025$ the intensity of these new components increases appreciably and at $x = 0.05$ a very broad spectral distribution with a plateau appears as a consequence of the superposition of three or more lines. Therefore, for $x > 0.01$ the crystals are not a homogeneous phase.

The N–Inc and Inc–C transitions in $(Cs_{1-x}Rb_x)_2ZnI_4$ crystals were studied earlier by NQR in the range of concentrations x between 0 and 0.025. The N–Inc and Inc–C transitions were clearly observed at the concentrations corresponding to the random distribution of Rb ions. The N–Inc transition region at $x = 0.025$ is very wide. The line broadening and the additional lines observed at this concentration prevent us from showing exactly the Inc–C transition temperature; however, the transition is observable. The concentration $x = 0.025$ was determined in [10] as exceeding the limit of Rb content consistent with a homogeneous phase in the series of solid solutions $(Cs_{1-x}Rb_x)_2ZnI_4$. We later measured the crystal with $x = 0.05$. Both transitions can still be discerned, with difficulty, from the noisy background.

2.3. X-ray study

The x-ray studies on the doped crystals with concentrations $x = 0.010$, 0.025 and 0.05 were performed using a four-circle diffractometer (Nonius CAD-4) equipped with a fine-focus Mo x-ray tube and a graphite monochromator ($\lambda_{\text{Mo K}\alpha} = 0.710\,73$ Å). The temperature was controlled using a Nonius FR558 cryostat, which regulates temperature to within ± 1 K. The satellite reflections are present only around Bragg reflections ($h60$) with $h = 2n$. The diffraction patterns were obtained as q-scans along the reciprocal line ($h60$), as was done in pure Cs_2ZnI_4 [11]; that is, the q-vector was parallel to the reciprocal axis $\boldsymbol{a}^*$. During the q-scan measurements, the diffracted beam was screened using the 0.2 mm wide vertical slit of the aperture/filter unit of the diffractometer, with a crystal-to-slit distance of 173 mm. Stationary counts were made at each point along the q-scan, with step widths Δh calculated so as to give a 0.002 Å^{-1} displacement between points. This value corresponds roughly to the scan length subtended at the centre of the crystal by the 0.2 mm vertical slit.

The incommensurate misfit parameter Δ was determined from the positions of the satellite reflections $(-3/2 - \Delta, 6, 0)$; $(-1/2 - \Delta, 6, 0)$; and $(3/2 + \Delta, 6, 0)$; $(1/2 + \Delta, 6, 0)$ with respect to the Bragg reflections $(-2, 6, 0)$; $(0, 6, 0)$ and $(2, 6, 0)$, respectively. The temperature dependence of the Δ-value, averaged over the four satellite positions, is presented in figure 4. The curve for $x = 0$ is taken from figure 3 of [11]. The misfit parameter for $x = 0$ decreases monotonically from 0.137 at $T_I = 117$ K to 0.069 at 108 K and then changes abruptly to $\Delta = 0$ at T_L. The Δ-dependences at different Rb contents show a shift in the temperature scale, in accordance with the x–T phase diagram (figure 2). The qualitative behaviour of Δ does not change noticeably within the experimental error. The phase transition is clearly observed at all x concentrations. In the vicinity of the transition point the satellites are split into two components with wavevectors $\boldsymbol{q} = 1/2\boldsymbol{a}^*$ and $\boldsymbol{q}_\Delta = (1/2 + \Delta)\boldsymbol{a}^*$. However, the temperature stability in our experiments was not good enough to allow a quantitative estimation of the breadth of the temperature region where coexistence occurs. The same holds true for the value of Δ in the gap, which appears not to change noticeably for different values of x. After the transition into the normal phase, the incommensurate satellites broaden sharply, transforming into diffuse spots.

The reflections ($hk0$) with $h = 2n + 1$ are systematically absent in the initial *Pnma* phase. In the doped crystals, however, we observe the weak reflections $(-1, 6, 0)$ and $(1, 6, 0)$ in the diffraction pattern at room temperature. The space-group-forbidden reflections have comparable intensities for all of the Rb-ion concentrations studied. One should note that reflections at the positions of $(-1, 6, 0)$ and $(1, 6, 0)$ are allowed for a modification of the present structure having space group $P2_1/m$ and with the $\boldsymbol{a}$-axis of the unit cell doubled [11]. Measurements of the reflection intensities in the ($hk0$) net out to $2\theta = 50°$ for $x = 0.01$ and to $2\theta = 55°$ for $x = 0.025$, figure 5, show that the reflections with $h \neq 2n$ are systematically very weak, although some are above background. It is likely that the intensities at these locations are

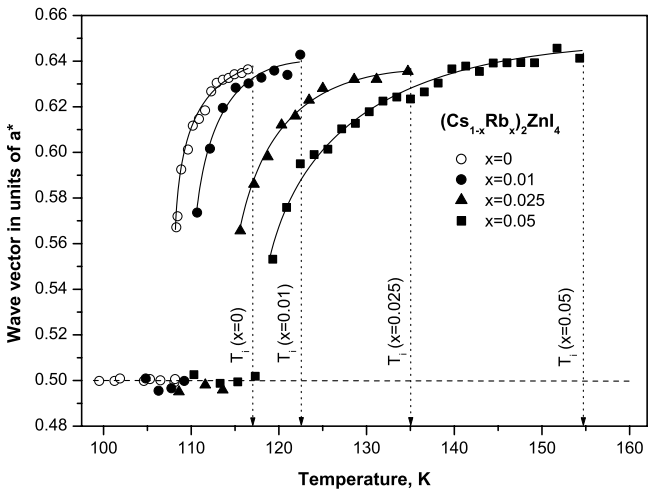

Figure 4. The temperature dependence of the wavevector $q_\Delta = (1/2 + \Delta)a^*$ for $(Cs_{1-x}Rb_x)_2ZnI_4$ ($x = 0$, 0.01, 0.025 and 0.05); dashed arrows indicate the T_I temperature as determined from the NQR measurements.

caused by factors other than Bragg scattering, and that the space group is still best described as *Pnma*. The structure of the sample with $x = 0.050$ was found to be isotypic with the structure for β-K_2SO_4 [12]. The space group, *Pnma*, is the same for both structures. While the unit-cell constants differ markedly ($a, b, c = 10.7622(14)$, 8.3087(7), 14.4327(19) Å for $(Cs_{1-x}Rb_x)_2ZnI_4$ and $a, b, c = 7.476(3)$, 5.763(2), 10.071(4) Å for β-K_2SO_4), the positions of analogous atoms within the cell are similar for the two structures; and the cell length ratios (a:b:c) for a *Pnma* setting are (0.746:0.576:1.00) for $(Cs_{1-x}Rb_x)_2ZnI_4$ and (0.742:0.572:1.00) for β-K_2SO_4. Thus, the structure of the sample with $x = 0.050$ is also isotypic with the end-member Cs_2ZnI_4.

In the pure compound, either grown from a melt or from a solution, we could not discern the fourth transition reported to occur at 104 K [13] by any of the techniques employed in this work. The doped compounds did not show that transition either.

3. Thermodynamic analysis

The difference in the effective charges and radii of the substitution (Rb) and host (Cs) ions in our case is small; however, the end members of the solid solution series, Cs_2ZnI_4 and Rb_2ZnI_4, are not isomorphic. The NQR and x-ray measurements show that in the range of $x \leqslant 0.01$ the substitution is random and does not break the symmetry of the normal phase. It seems to generate defects of so-called 'random local transition temperature' type at these concentrations. This type of defect usually shifts the transition temperatures and smears (broadens) the anomalies of physical quantities. Basically, we shall assume that the systems can be considered as homogeneous.

In the case of a homogeneous system that undergoes successive N–Inc–C transitions, with the commensurate modulation $\boldsymbol{q}_C = 1/2\boldsymbol{a}^*$, the essential part of the thermodynamical functional f is

$$f(x) = \frac{\alpha}{2}\rho^2 + \frac{1}{4}\beta_1\rho^4 - \frac{1}{4}\beta_2\rho^4\cos(4\theta) - \delta\rho^2\dot{\theta} + \frac{\kappa}{2}(\dot{\rho}^2 + \rho^2\dot{\theta}^2) \qquad (1)$$

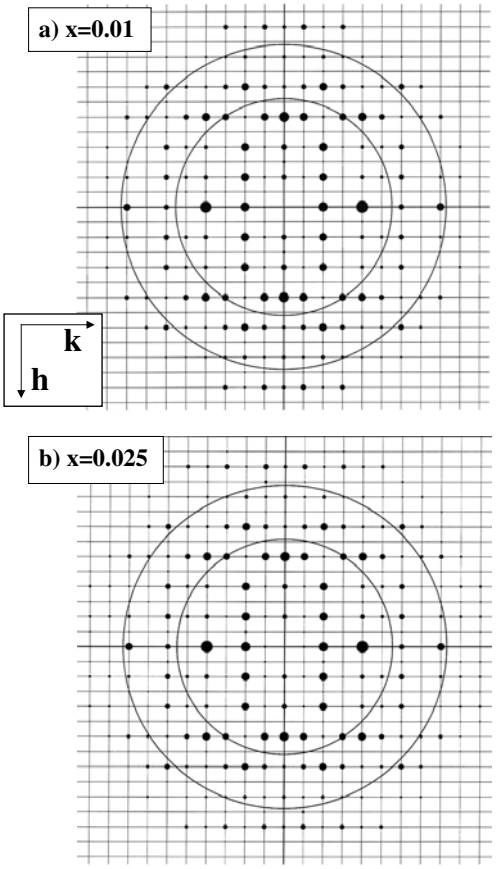

Figure 5. Representations of diffracted intensity in the $(hk0)$ plane for $(Rb_xCs_{(1-x)})_2(ZnI_4)$, with $x = 0.010$ (a) and $x = 0.025$ (b). The index h runs vertically downward from $h = 0$ at the centre of the drawing in each case, and k increases to the right beginning with $k = 0$ at the centre. The circles represent resolutions of 1.50 (inner) and 1.00 Å.

in terms of the two-dimensional order parameter $Q = \rho(z)e^{i\theta(z)}$ where the amplitude and phase contain the position dependence [14, 15]. The first three terms are characteristic of crystals with a low-symmetry commensurate phase, the fourth term is the Lifschitz invariant which stabilizes the incommensurate phase and the fifth term tends to inhibit it. $\dot{\theta}$ and $\dot{\rho}$ are the derivatives with respect to the spatial coordinate z.

The free energy functional, the order parameter and the spatial coordinate can be scaled as $f = \beta_1\gamma^4 f^*$, $\rho = \gamma\rho^*$ and $x = \kappa z^*/\delta$, with $\gamma = \delta/\sqrt{\kappa\beta_1}$.

The scaled energy density $F(\alpha^*, r)$ then depends on only two parameters, the anisotropy parameter $r = \beta_2/\beta_1$ and the $\alpha^* = \kappa\alpha/\delta^2$ [16].

We shall assume that the substitution of Rb has two main consequences in the free energy of the crystal.

The anisotropy parameter, r, changes when the Rb concentration, x, changes, but remains homogeneous in the entire crystal and can be determined from experiment using expression (4) (see below). This approach is similar to the 'virtual-crystal approximation' which has been used previously to analyse the x dependence of the N–Inc–C transitions in $[(CH_3)_4N]_2CuBr_xCl_{4-x}$ [17].

It is assumed that at fixed concentration $\alpha^* = \alpha_0^*(T - T_0)$, with T_0 the hypothetical commensurate phase transition temperature in the absence of the fourth and fifth terms in f, and that r, the anisotropy parameter, does not depend on T.

To calculate the average free energy we have followed the variational method in which the average potential F is minimized with respect to both q and θ at given temperature, and yields their equilibrium values [16].

The average potential in the normal, $F_N(\alpha^*)$, and commensurate, $F_C(\alpha^*)$, phases can be calculated analytically, giving

$$F_N(\alpha^*) = 0 \qquad \text{and} \qquad F_C(\alpha^*) = -\alpha^* 2/(4(1-r))$$

while the incommensurate phase, $F_I(\alpha^*)$ has to be calculated numerically.

For fixed concentration, the N–Inc transition, when $F_N(\alpha_I^*) = F_I(\alpha_I^*)$, occurs at $\alpha_I^* = 1$, and presents a steplike anomaly with

$$\Delta C_p(T_I) = \frac{\alpha_0^2}{2\beta_1}. \tag{2}$$

To calculate the lock-in transition temperature T_L, when $F_I(\alpha_L^*) = F_C(\alpha_L^*)$, needs a numerical solution.

Besides, in the commensurate transition the excess heat capacity just below T_L obeys the relation

$$\Delta C_p(T_L) = \frac{\alpha_0^2}{2\beta_1(1-r)}. \tag{3}$$

From (2) and (3) the coefficient r can be calculated:

$$r = 1 - \frac{T_L/T_I}{\Delta C_p(T_L)/\Delta C_p(T_I)}. \tag{4}$$

We note that the determination of r by this procedure only requires us to know the values of the relative heat capacity anomalies. Consequently, our ac relative measurements give the necessary information to apply this equation (see table 1).

4. Discussion

The crystals of the A_2BX_4 family represent the 'model' case for the application of the continuum theory to the interpretation of incommensurate phase transitions. The two-component order parameter transforms as the two-dimensional irreducible representation of the symmetry group of the N phase *Pnma*. The incommensurate modulation arises along a single direction. In the constant-amplitude approximation the structure of the Inc phase can be described in terms of a soliton lattice except in the vicinity of the N–Inc transition, in the single-harmonic limit [18]. The idea of the soliton lattice has been successfully used to explain very specific phenomena near the Inc–C transition observed in the presence of point defects. Near the transition the intersoliton distance L diverges logarithmically to ∞ and intersoliton interaction becomes so weak that the phase of the modulation is determined by the field of defects. The randomly distributed defects work as traps for the periodicity, then, the long range order of a soliton lattice is destroyed by the strong 'pinning' of the modulation wave by impurities. The longer L and the narrower the solitons the larger the pinning energy. Sometimes the natural content of impurities in the crystal is sufficient to induce a steplike behaviour of q_Δ near the lock-in transition. The values of q_Δ at the steps depends on the path to the measuring point on the pressure–temperature phase-plane [9]. The pinned wavevector values in q-domains correspond to non-equilibrium states. When the temperature is changed the modulation period must take a new equilibrium value corresponding to the new temperature.

However, defects prevent such processes from proceeding freely. In all known cases a well defined thermal hysteresis, which rapidly increases with the impurity concentration, has been observed by measurements of the modulation wavevector or via the temperature behaviour of different physical properties near the Inc–C transition.

In the context of this paper it is interesting to remember the results of the heat capacity and incommensurate wavevector study in the $(Rb_{1-x}K_x)_2ZnCl_4$ system [6, 7] which may be considered as a classical scenario for the Inc-modulation evolution at different concentration of the substituted ions. Both end members in the solution range investigated are isomorphous to each other and undergo the same type of N–Inc–C transition. The differences in the effective charge and radii of the host and substituted ions were chosen to be small to reduce side effects to the minimum. The substitution does not break the symmetry of the normal phase until a large concentration of substitutes is introduced in the lattice. The heat capacity data in the $(Cs_{1-x}Rb_x)_2ZnI_4$ system look similar to those observed in the $(Rb_{1-x}K_x)_2ZnCl_4$ system. The N–Inc transition temperature lies on a straight line connecting the T_I values for the pure K and Rb compounds. The substitution widens this transition somewhat but does not change the shape of the heat capacity anomaly. In contrast, the Inc–C transition is essentially blurred by substitution. At intermediate concentrations (for example at $x = 0.02$) the Inc–C heat capacity anomaly is still observable. The behaviour of the satellite reflections near the transition becomes very complicated, showing the coexistence of metastable states with slightly different q-values. The thermal hysteresis of the Inc–C transition is about 30 K. For larger defect concentration, in the range $0.1 \leqslant x \leqslant 0.9$, the heat capacity anomaly at T_L is completely suppressed and does not show any sign of the Inc–C transition. The modulation wavevector q_Δ is fixed at the value found at T_I over the whole temperature range below T_I. The metastable Inc state is observed until the lowest investigated temperature.

As it is very easy to see from the temperature dependence of q_Δ (figure 4) our system does not follow the expected scenario in spite of the heat capacity data looking very similar to that quoted above. The Inc–C transition is clearly observed on the temperature dependence of q_Δ at all Rb concentrations including the largest ones $x = 0.025$ and 0.05 when the heat capacity anomaly is already smeared. The substitution does not apparently change the character of the wavevector temperature dependence. Only at the maximal concentration $x = 0.05$ can one perceive some hint of non-monotonic q_Δ behaviour in the Inc region. Unfortunately the available x-ray diffractometer was not specially equipped for a very precise scanning of the q-space. Thus, information on metastable modulations which possibly coexist close to the Inc–C transition may be lost. Nevertheless, the obtained results certainly show that the smearing and disappearance of the heat capacity anomaly at the Inc–C transition in our system is not connected with strong non-equilibrium processes of the phase modulation pinning. We have not observed either a clear demonstration of these processes, such as thermal hysteresis of the Inc–C transition, which usually increases rapidly with x. This is the first case, to our knowledge, where the interaction of the modulation with defects is so weak even near the Inc–C transition.

Both the structure of the 'host' crystal in the N phase and the kind of defect generated by the Rb substitution at small x are of the same type as in the earlier studied $(A_{1-x}A'_x)_2BX_4$ solid solutions. In spite of these similarities the incommensurate phase in Cs_2ZnI_4 has certain special features. The anisotropy invariant $r\rho^n \cos n\theta$ in the thermodynamic potential has the integer $n = 6$ for most of the A_2BX_4 crystals. In Cs_2ZnI_4 this integer characterizes the two-dimensional representation; it is equal to 4 in accordance with the doubling of the unit cell parameter of the N phase below the T_L. The approximation of the soliton lattice is well applicable in the case of weak anisotropy realized in $n = 6$ systems. For $n = 4$ the anisotropy is not necessarily weak [19]. Cs_2ZnI_4 is exactly the case of the middle anisotropy condition

where $r \cong 0.45$ as was shown in [15, 16]. In the studied series of the $(Cs_{1-x}Rb_x)_2ZnI_4$ solutions the parameter r is varied between 0.50 and 0.33. In that case the solution for the order parameter near Inc–C transition is neither solitonic nor truly sinusoidal [16]. The absence of the well formed narrow solitons near T_L is a critical condition against the presence of a strong pinning by defects in this region. Additionally one should note that our thermodynamic prediction overestimates the expected values of the hysteresis; indeed, the supercooling at $x = 0$ is estimated as 7 K, while experimentally the coexistence region of commensurate and incommensurate modulations at T_L does not exceed 0.6 K in Cs_2ZnI_4 [11]. Recent x-ray data [20] show that in Cs_2ZnI_4 the interplanar distances and the unit-cell volume do not exhibit measurable jumps at the Inc–C transition. The overestimation of the first-order nature of the Inc–C transition in our case may be due to the restriction by the fourth-order terms on the order parameter in the expansion (1).

The heat capacity anomaly at T_L moderately widens, maintaining the outline of the original shape in the region of x where the NQR shows the random distribution of the Rb ions. No randomization factor was introduced in our thermodynamic description, in fact the random distribution was considered to act homogeneously on all parameters. The observed broadening of the C_p anomaly at T_L in the range of $x \leqslant 0.01$ may be explained, in principle, by the mechanism known for usual commensurate three-dimensional crystals with a one-component order parameter and non-symmetry-breaking impurities [21].

For $x = 0.025$ and 0.05 the NQR spectrum shows that the distribution of the defects is no longer random. In the system under study the end members of the solid solution series are not isomorphic substances; Rb_2ZnI_4 is monoclinic at room temperature [22]. Thus mixed crystals do not form a continuous series of solid solutions. Usually there exists a range of x where the mixed crystals are not homophase. As is well known from the numerous studies of solid solutions with diffuse phase transitions a violation of the random distribution of impurities leads to very abrupt blurring of the physical property anomalies (e.g. [23]). We suppose that the change in the regime of the interaction between the matrix and defects is responsible for the smearing of the Inc–C heat capacity anomaly at the large Rb concentrations in our crystals. The loss of homogeneity generates elastic strains which in all probability lead to the suppression of the low-temperature first-order transition.

Since Cs_2ZnI_4 is an improper ferroelastic the possible contribution of fluctuations in heat capacity anomalies should be noted. However at $x = 0$ the influence of fluctuations is negligible as was mentioned in [15, 16]. In the substituted crystal one can expect an increase of the fluctuation contribution resulting from the decrease of the correlation radius of fluctuations far from the transition point (see e.g. [25]). The local modes may also contribute to C_P anomalies and simultaneously broaden them. Our measurements in contrast show the subsequent decrease of the C_P value at T_L with the growing content of Rb. The second-order anomaly at the N–Inc transition maintains the steplike shape at all x.

Note that the shifts of the N–Inc and Inc–C phase transitions with x in the higher-temperature side (figure 2) are in agreement with common regularity established for A_2BX_4 structures [25, 26]. As shown, the factor determining the stability of these structures is the height of the potential barriers preventing a certain kind of tetrahedral group motion. The low-temperature transition has the opposite sign of temperature shift with x. Most probably it is not caused by the ordering of the tetrahedral groups and has a displacive nature.

5. Conclusion

In the present work the solid solutions of the $(Cs_{1-x}Rb_x)_2ZnI_4$ series have been studied experimentally using AC-calorimetric and x-ray measurements. The x–T phase diagram has

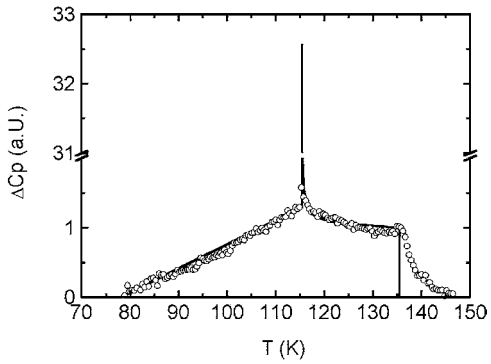

Figure 6. Calculated $\Delta C_p(T)$ with parameters given in the (table 1), compared to experimental data for $x = 0.025$.

been determined in the range of Rb concentration between $x = 0$ and 0.05. The variational model used allows us to describe the transition for low concentrations of Rb as due to a reduction of the anisotropy r. The calculated heat capacity peaks, however, remain narrow and too high, while the experimental anomalies broaden with the Rb content (figure 6). This discrepancy already appears in the pure compound and becomes larger for larger concentrations of doping. One should note that it is a natural consequence of the approach that takes account of the influence of the substitution effectively only through the variation of the parameters for a homogeneous system. The moderate broadening of the heat capacity anomalies in the range of x where a distribution of Rb is random can be explained as in usual crystals doped with non-symmetry-breaking impurities. At the concentrations $x > 0.01$ a rapid smearing of the Inc–C anomaly is connected with the violation of the random distribution of defects. In our opinion, the most interesting results are the facts showing unusually weak interaction of the incommensurate modulation with point defects even in the region close to the Inc–C transition. We have not detected any temperature hysteresis, irrespective of the amount of substitution in this region. The thermodynamic description shows that $(Cs_{1-x}Rb_x)_2ZnI_4$ crystals correspond to the case of an intermediate anisotropy in the thermodynamic potential when the solution for the order parameter is not solitonic near the Inc–C transition. In that case the energy of the pinning may be too weak to fix the modulation.

Acknowledgments

This paper is dedicated to Professor Dr Domingo Gonzalez from the University of Zaragoza on the occasion of his retirement. This work has been partially financed with projects CICYT MAT99/1142 and the INTAS-97-10177. The authors thank A P Levanyuk for useful discussion of the results.

References

[1] Lee P A and Rice M J 1979 *Phys. Rev.* B **19** 3970
[2] Imry Y and Ma S 1975 *Phys. Rev. Lett.* **35** 1399
[3] Lebedev N I, Levanyuk A P and Sigov A S 1987 *Sov. Phys.–JETP* **65** 140
[4] Bak P and Pokrosky V L 1981 *Phys. Rev. Lett.* **47** 958
[5] Hamano K, Ikeda Y, Fujimoto T, Ema K and Hirotsu S 1980 *J. Phys. Soc. Japan* **49** (Suppl. B) 10

[6] Hamano K 1986 *Incommensurate Phases in Dielectrics: 1. Fundamentals* ed R Blinc and A P Levanyuk (Amsterdam: North-Holland) ch 9
[7] Mashiyama H, Tanisaki S and Hamano K 1981 *J. Phys. Soc. Japan* **50** 2139
Mashiyama H, Tanisaki S and Hamano K 1982 *J. Phys. Soc. Japan* **51** 2548
[8] Iizimi M and Gesi K 1983 *J. Phys. Soc. Japan* **52** 2526
[9] Parlinsky K, Currat R, Vettier C, Aleksandrova I P and Eckold G 1992 *Phys. Rev.* B **46** 106
[10] Sukhovskii A A, Lisin V V, Aleksandrova I P, Voronov V N and Melero J J 1999 *Phys. Solid State* **41** 128
[11] Bagautdinov B Sh and Aleksandrova I P 1994 *Solid State Commun.* **90** 817
[12] McGinnety 1972 *Acta Crystallogr.* B **28** 2845
[13] Díaz-Hernandez J, Tello M J, Igártua J M, Ruiz-Larrea I, Breczewski T and Lopez-Echarri A 1995 *J. Phys.: Condens. Matter* **7** 7481–7
[14] Ishibashi Y 1986 *Incommensurate Phases in Dielectrics: 2. Materials* ed R Blinc and A P Levanyuk (Amsterdam: North-Holland) ch 11
[15] Melero J J, Bartolomé J, Burriel R, Aleksandrova I P and Primak S 1995 *Solid State Commun.* **95** 201
[16] Jacobs A E 1996 *J. Phys.: Condens. Matter* **8** 517
[17] Liechti O and Kind R 1991 *Phys. Rev.* B **44** 7209
[18] Levanyuk A P 1986 *Incommensurate Phases in Dielectrics: 1. Fundamentals* ed R Blinc and A P Levanyuk (Amsterdam: North-Holland) ch 1
[19] Sannikov D G 1986 *Incommensurate Phases in Dielectrics: 1. Fundamentals* ed R Blinc and A P Levanyuk (Amsterdam: North-Holland) ch 2
[20] Bagautdinov B Sh and Shekhtman V Sh 1999 *Phys. Solid State* **41** 123
[21] Levanyuk A P and Segov A S 1988 *Defects and Structural Phase Transitions* (New York: Gordon and Breach) ch 11
[22] Mashiyama H M, Takesada M, Kojima M and Kasano H 1994 *Ferroelectrics* **152** 313
[23] Lines M E and Glass A M 1997 *Principles and Applications of Ferroelectrics and Related Materials* (Oxford: Clarendon) ch 8
[24] Strukov B A and Levanyuk A P 1983 *Fizicheskie Osnovy Segnetoelektricheskikh Yavleniy v Kristallakh (The Physical Basis of Ferroelectric Phenomena in Crystals)* (Moscow: Nauka) pp 118–20
[25] Subramanian R K, Venu K and Sastry V S S 1995 *J. Phys.: Condens. Matter* **7** 3033
[26] Kolinsky C, Jannin M, Puget R, Delarue P and Godefroy G 1997 *J. Phys.: Condens. Matter* **9** 825